Effect of 10-Year Outdoor Exposure and Curing Conditions on the Pore Structure Characteristics of Hardened Cement Mortar

Nguyen Xuan Quy, Junho Kim and Yukio Hama

Pore Structure Model of Hydrates Comprising Various Cements and SCMs Based on Changes in Particle Size of Constituent Phases
Yusuke Fujikura, Hideki Oshita
Journal of Advanced Concrete Technology, volume 9 (2011), pp.133-147.

Influences of PCE Superplasticizer on the Pore Structure and the Impermeability of Hardened Cementitious Materials
Yanrong Zhang, Xiangming Kong
Journal of Advanced Concrete Technology, volume 12 (2014), pp.443-455.

Characterizing the 3D Pore Structure of Hardened Cement Paste with Synchrotron Microtomography
Michael Angelo B. Promentilla, Takafumi Sugiyama, Takashi Hitomi, Nobufumi Takeda
Journal of Advanced Concrete Technology, volume 6 (2008), pp.273-286.

Effect of 10-Year Outdoor Exposure and Curing Conditions on the Pore Structure Characteristics of Hardened Cement Mortar

Nguyen Xuan Quy[1], Junho Kim[2] and Yukio Hama[3*]

Abstract

The objective of this study was to determine the influence of environmental conditions on the pore structure of mortar. For this purpose, the experimental program was designed with the following two series: Series 1 included both a 10-year outdoor exposure test set and a laboratory test set and Series 2 included only a laboratory test set. The pore structure of mortar specimens was evaluated using the Mercury Intrusion Porosimetry method. In general, the pore structure change due to temperature in both the outdoor exposure test and the laboratory test showed the same tendency. The test results confirmed that the pore structure of mortar coarsened and that the volume of pores with a diameter range of 40 to 2000 nm increased due to the increase in temperature and the decrease in relative humidity. Furthermore, this paper reports evidence for the relationship between pore structure change and maturity, and an improved maturity function is proposed. The change in the pore structure is determined by the proposed maturity function, which considers the curing temperature history and the relative humidity. The relative humidity is an additional and novel factor forming the new maturity function for the prediction of pore structure change.

1. Introduction

For a variety of reasons, pore structure has become the focus of modern building material science and has received much attention for many years. Cement-based materials are porous materials; thus, pore structure characteristics play a critical role in the engineering properties of cement-based materials (Mehta and Monteiro 2014). Knowledge of the pore structure change is useful for exercising control on the durability properties and for predicting the deterioration behavior, such as frost damage and carbonation, of cement-based materials (Neville 2012; Taylor 1997).

Much research in recent years has focused on the examination of the pore structure change of cement-based materials using the Mercury Intrusion Porosimetry (MIP) method (Aono *et al*. 2006; Atarashi *et al*. 2009; Choi *et al*. 2017; Diamond 2000; Gallé 2001; Gao *et al*.

2016; Nakamura *et al*. 2015a; Nakamura *et al*. 2015b; Winslow and Liu 1990), which has become an important tool for studying pore structure (Aligizaki 2006; Lamond and Pielert 2006; Scrivener *et al*. 2016). Changes in the pore structure of cement-based materials such as mortar can modify the engineering properties (Marusin 1981; Maruyama *et al*. 2017; Parrott 1992). Previous results showed that the change in the pore structure of hardened cement paste is probably related to the change in the nanostructure of the C-S-H gel, which is a main constituent of the hardened cement paste (Kamada *et al*. 1996; Powers 1958; Powers and Brownyard 1946). It was pointed out recently that the nanostructure of the C-S-H and the micro-pore structure of concrete are remarkably changed by drying or drying–wetting cycles (Chang *et al*. 2017; Parrott 1981). In addition, the change in the micro-pore structure is due to the polymerization of silicate anions coordinated with a CaO layer developed when the C-S-H was subjected to drying (Aono *et al*. 2007; Espinosa and Franke 2006). In spite of these efforts, the effects of different environmental conditions on the pore structure change in the mortar are not fully understood. Moreover, the ambient conditions, such as the temperature and humidity during the in-laboratory drying period, might be different from actual ambient conditions in the outdoor exposure environment. Therefore, it is of great significance to evaluate the pore structure changes in outdoor exposure tests for mortar samples (Tonoli *et al*. 2011; Zhang and Zhang 2006).

The main factors affecting the pore structure change of mortar are age, relative humidity, mix proportion parameters, and curing temperature. Espinosa and Franke (2006) showed that the surface area of hardened Portland cement paste reduces after chemical aging

[1]PhD candidate, College of Environmental Technology, Graduate School of Engineering, Muroran Institute of Technology, 27-1 Mizumoto, Muroran 050-8585, Japan. Department of Building Material Technology, Faculty of Civil Engineering, Hanoi Architectural University, Hanoi, Vietnam.
[2]Postdoctoral Researcher, College of Environmental Technology, Graduate School of Engineering, Muroran Institute of Technology, 27-1 Mizumoto, Muroran 050-8585, Japan.
[3]Professor, College of Environmental Technology, Graduate School of Engineering, Muroran Institute of Technology, 27-1 Mizumoto, Muroran 050-8585, Japan.
*Corresponding author,
E-mail: hama@mmm.muroran-it.ac.jp

Table 1 Physical properties and chemical composition of OPC.

Series	Specific gravity (g/cm³)	Specific surface (cm²/g)	Mineral composition (Rietveld) (%)				
			C_3S	C_2S	C_3A	C_4AF	Others
1	3.16	3460	60.2	16.2	4.7	5.4	13.5
2	3.15	3510	68.7	11.7	7.5	5.5	6.6

Table 2 Mix proportions.

Series	Water-cement ratio (W/C)	Sand-cement ratio (S/C)	Material contents (kg/m³)			Flow (cm)
			Water	Cement	Sand	
1	0.35	2.0	248	709	1418	15
	0.55		342	621	1242	28
2	0.35	2.0	247	706	1412	16
	0.45		297	660	1320	23
	0.55		340	619	1238	29

while the pore structure becomes coarser due to the drying process. Adolphs *et al*. (2002) found that the changes in the mesoporous range (10 nm to 100 nm) of hardened cement paste exhibits a strong dependency on relative humidity (RH). Hamami *et al*. (2012) determined that the water-to-cement mass ratio and paste volume fraction were the main mix parameters affecting porosity. Moukwa and Aïtcin (1998) pointed out that the oven-drying temperature affects the pore structure of hardened cement paste by opening pores in the range of 0.02 and 0.1 μm. The influence of heat curing on the pore structure was also identified by Reinhardt and Stegmaier (2006) and Galan *et al*. (2016). Furthermore, a maturity function is defined in ASTM C1074 - 11 as follows: "a mathematical expression that uses the measured temperature history of a cementitious mixture during the curing period to calculate an index that is indicative of the maturity at the end of that period". In addition, the maturity is a function of the product of the temperature multiplied by time (ACI 116R). As a result, it is believed that the pore structure change is closely related to the maturity function (Nakamura *et al*. 2015a; Nakamura *et al*. 2015b).

The term "maturity" was introduced for the first time in 1951 (Saul 1951), and is calculated from the temperature history according to the Nurse-Saul maturity function shown in Eq. 1,

$$M = \sum_{0}^{t} (T - T_0) \Delta t \tag{1}$$

where M is the maturity index (°C-days), T is the average concrete temperature (°C), T_o is the datum temperature (°C), t is the elapsed time (days), and Δt is the time interval (days).

Eq. 1 shows the time-temperature relationship which is called maturity function. This function takes only the effect of temperature on the strength development of concrete into account and has mostly been used with the cold weather concreting.

Although there are many studies related to this maturity method (Abdel-Jawad 2006; Carino and Tank 1992; Galobardes *et al*. 2015; Jin *et al*. 2017; Liao *et al*. 2008;

Malhotra and Carino 2004; Meneghetti and Meneghetti 1985; Topçu and Toprak 2005; Voigt *et al*. 2006; Volz *et al*. 1981; Xuan *et al*. 2018; Yikici and Chen 2015), they have mostly focused on strength–maturity relationships for concrete; little attention has been paid to the pore structure–maturity relationships for mortar particularly (Nakamura *et al*. 2015b). Moreover, literature on the relationship between the maturity and pore structure change is rare and little evidence is available.

Therefore, in this study, the influence of the environmental conditions, i.e., the temperature and relative humidity, on the pore structure of mortar is investigated. Mortar specimens were prepared and subjected to drying conditions in the laboratory and exposed to different real natural climate conditions. The experimental results show that the pore volume changed significantly due to changes in the environmental conditions. Based on the pore volume change of the pores of diameter 40–2000 nm, a modified maturity function that is able to predict the change in the mortar pore structure caused by environmental conditions is proposed. The results of this study strongly confirm previous predictions about the relationship between maturity and pore structure change.

2. Materials and methods

2.1 Materials
Ordinary Portland cement (OPC) in accordance with Japanese Industrial Standard was used to make the mortar in Series 1 and 2. The physical properties and mineral compositions are given in **Table 1**. The mineral composition of the OPC was quantified by the X-ray diffraction (XRD) Rietveld method. The sand used as fine aggregate was obtained from a natural origin. The properties of the fine aggregates were determined as follows: the total water absorption was 1.52%, the density at a saturated and surface-dried condition (SSD) was 2698 kg/m³, the bulk density was 1487 kg/m³, and the fineness modulus was 2.6.

Table 2 shows the proportions to prepare the mortar samples in Series 1 and Series 2. In Series 1, the main mix variables were the free water-to-cement mass ratio (W/C) of 0.35 and 0.55 and the sand-to-cement ratio

Table 3 Experimental in-laboratory plan.

Series	Symbols	Initial curing	Environmental conditions after initial curing		Time interval (weeks)
			Temperature (°C)	Humidity (%)	
1	4WK	Water curing at 20 ℃ for 4 weeks	-	-	-
	20D-4W		20	60	4
	50DL-2W		50	5	2
	50DL-4W		50	5	4
	50DH-2W		50	60	2
	50DH-4W		50	60	4
	50DW-2W		Dry/Wet cycles (*)		2 (4cycles)
	50DW-4W				4 (8cycles)
2	20ºC-23%RH	Water curing at 20 ℃ for 4 weeks	20	23	0, 2, 4, 8, 13, 26
	20ºC-60%RH		20	60	
	20ºC-75%RH		20	75	
	20ºC-100%RH		20	100	
	35ºC-13%RH		35	13	
	35⁰C-60%RH		35	60	
	50ºC-6%RH		50	6	
	50ºC-23%RH		50	23	
	50ºC-60%RH		50	60	
	50ºC-75%RH		50	75	
	50ºC-100%RH		50	100	
	50ºC-DW		Dry/Wet cycles (*)		

(*) 1 Dry/Wet cycle = Drying at 50℃ (5% RH) for 3 days then wetting at 50℃ for 0.5 day.

(S/C) of 2 : 1 without any chemical admixture. In Series 2, the main mix variables were W/C of 0.35, 0.45, and 0.55 and with the same S/C as that of Series 1.

2.2 Methods
(1) Preparation and curing of mortar specimens
The materials were mixed in a pan mixer. The cement and fine aggregate were mixed first. After the materials were uniformly dispersed, water was added and mixed until a consistent mixture was obtained.

For each mortar mixture, $40 \times 40 \times 160$ mm prisms were cast. After casting, all the prisms were left in the casting room and covered with plastic sheeting for approximately 24 h. They were then demolded and cured in the laboratory and outdoor exposure sites according to the experimental program.

(2) Experimental program
The experimental program was designed for the following two series. In Series 1, one test set involved subjecting the mortar specimens to drying conditions in the laboratory and another test set involved exposing the specimens to different climate conditions at three outdoor locations. The experiment plan was conducted in the laboratory as shown in **Table 3**. After demolding, the specimens were cut into cubes of $40 \times 40 \times 40$ mm and subjected to initial curing. First, the initial curing was performed in water at 20°C for 4 weeks for all mortar specimens. Next, drying curing and drying–wetting curing were applied at 20°C and 50°C, respectively. In the case of drying at 50°C in controlled chamber, different relative humidity levels (5% RH and 60% RH) were used. The 5% RH level set up by controlled chamber. The 60% RH level was performed using Potassium Io-

dide (KI) which is saturated salt aqueous solution, and the drying period was varied from 2 and 4 weeks as well. Simultaneously, the outdoor exposure test was also performed. After 4 weeks of initial curing, the mortar specimens were exposed to different natural climate regions for 10 years at three outdoor sites in Japan: Muroran (M), Tokyo (T), and Okinawa (O) (see **Fig. 1**). The latitude and longitude of M, T, and O are (42° N/141° E), (35° N/139° E), and (26° N/127° E), respectively. Muroran (a city is located in the northernmost of Japan) has a much cooler climate than Tokyo and Okinawa, long and heavy snowfalls dominate in winter. Tokyo (the Japanese capital) has the weather is temperate, hot, humid and rainy in summer; the winter is the sunniest and driest season of the year and snowfall is sporadic; sometimes can be affected by typhoons. The climate of Okinawa (southern island of Japan) is subtropical, with no snowfall in winter, and long, hot, moist and rainy summers and especially is the most affected areas by typhoons. The annual mean temperature (°C) and the annual mean relative humidity (% RH) at the three outdoor sites were M (8.9°C, 81% RH), T (16.4°C, 60% RH), and O (23.4°C, 71% RH). The total experimental time in Series 1 was 10 years, after which the experiments in Series 2 were performed.

In Series 2, the experiments were only performed in the laboratory (see **Table 3**). After demolding, the mortar specimens were cut into 40 mm cubes and subjected to the initial curing for 4 weeks at 20°C in water. Next, the specimens were immediately placed in the secondary curing conditions in various environmental conditions for a period of 2, 4, 8, 13, or 26 weeks. In this stage, drying temperatures of 20°C, 35°C, and 50°C were applied to mortar specimens; the relative humidity

setting (% RH) corresponding to each drying temperature level were as follows: 23% RH, 60% RH, 75% RH, and 100% RH (in case of 20°C); 13% RH and 60% RH (in case of 35°C); and 6% RH, 23% RH, 60% RH, 75% RH, and 100% RH (in case 50 of °C). To reach 23% RH, 60% RH and 75% RH level, the saturated salt aqueous solutions were used: for 23% RH using Potassium Acetate (CH₃COOK); for 60% RH using Potassium Iodide (KI); for 75% RH using Sodium Chloride (NaCl). 100% RH condition was in water. The drying–wetting cycle was set at 50°C and 6% RH for 3 days and then at 50°C in water for 12 hours.

(3) Determination of pore structure
First, after curing under each environmental condition, the mortar specimens were cut into $5 \times 5 \times 5$ mm cubes, excluding the material within 1 cm of the surface. Next, they were soaked in acetone for 24 hours immediately to stop the hydration reaction of cement and then kept in D-drying conditions for 24 hours. **Figure 2 (a)** shows the D-drying apparatus. The temperature of a dry ice–ethanol bath in the trap of this apparatus was kept at

−78°C, the temperature at which the water vapor pressure was about 0.5 µHg. Finally, the pore size distributions of the mortar specimens were characterized using MIP. The MIP test was performed using the Pore Master33 (U.S. Quantachrome Corp.) according to JIS R 1655 with operation pressures of up to 228 MPa, corresponding to 6 nm of minimum pore diameter. **Figure 2 (b)** shows the MIP apparatus. The contact angle between the mercury and pore wall was 140° and the surface tension of the mercury was 0.4854 N/m.

3. Results and discussion

3.1 Effect of exposure and curing conditions on the pore size distribution of the mortar
As mentioned previously, the aim of the tests was to determine the pore size distribution using MIP. It was possible to obtain information about the pore structure change, which is observed in terms of the critical pore entry diameter of differential curves (Cook and Hover 1999). The critical pore entry diameter is one of three important parameters characterizing the pore structure
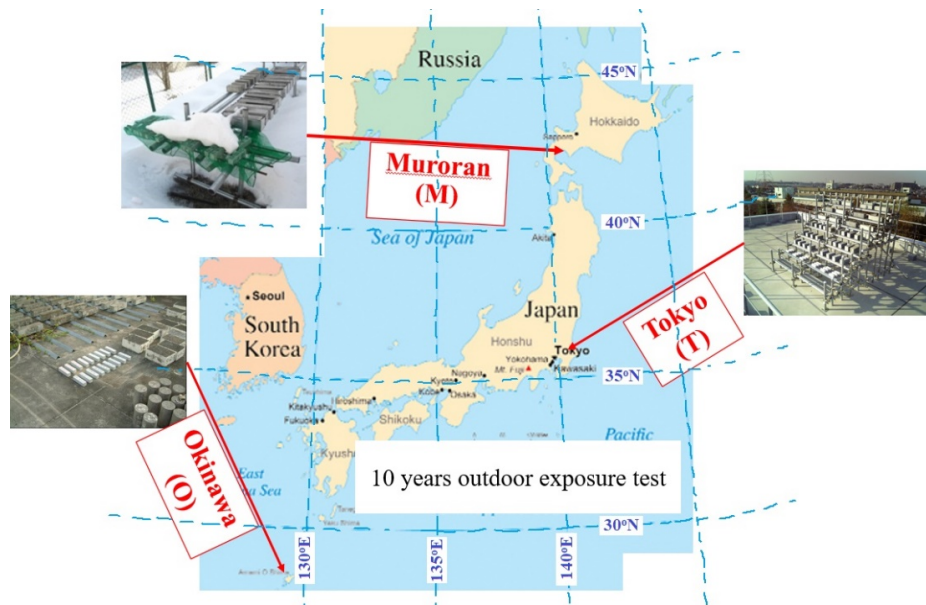

Fig. 1 Locations of outdoor exposure test on a map of Japan.

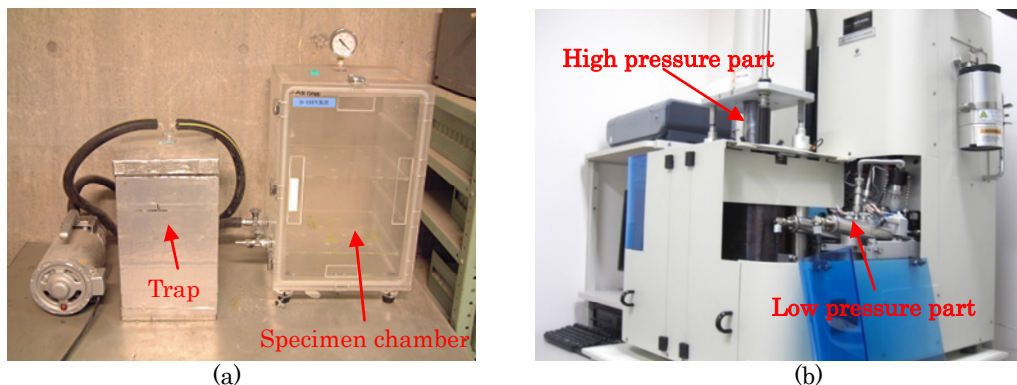(a)   (b)

Fig. 2 Testing equipment: (a) D-drying apparatus (b) Mercury Intrusion Porosimetry (Pore Master33, U.S. Quantachrome Corp.).

Table 4 The change of the critical pore entry diameters.

Sample	The critical pore entry diameters (nm)			
	Initial	1.5 years	5 years	10 years
OPC-0.35-M	32.19	9.19	9.64	9.83
OPC-0.35-T	32.19	43.2	46.48	145.58
OPC-0.35-O	32.19	85.03	95.22	69.2
OPC-0.55-M	62.15	57.92	155.41	162.09
OPC-0.55-T	62.15	65.64	171.81	29.06
OPC-0.55-O	62.15	153.21	195.41	205.28

(which are: total percolated pore volume, threshold pore entry diameter and critical pore entry diameter) can be determined from cumulative or differential curve of MIP results (see **Fig. 13**). Critical pore entry diameter is the pore diameter where the steepest slope of the cumulative curve is recorded (Scrivener *et al*. 2016). In the other way, critical pore entry diameter is the pore diameter corresponds to the highest peak of differential curve. **Figure 3** shows the curve of differential pore size distributions for OPC mortar (OPC-0.35 and OPC-0.55), which were measured at initial curing, and after 1.5, 5,

and 10 years of exposure in Series 1. The pore size distribution curves of OPC-0.35 and OPC-0.55 typically exhibit at least two sharp peaks. The critical pore entry diameter corresponding to highest peak in differential curve was showed in **Table 4**. These diameter of pore increased with increasing the W/C ratio. There was a slowdown and downward trend in the increasing of the critical pore entry diameter after 5 years exposure. A clear difference can be observed for the 1.5-, 5-, and 10-year exposure testing samples (see **Fig. 3**: OPC-0.35-M, OPC-0.35-T, and OPC-0.35-O, respectively). By com-
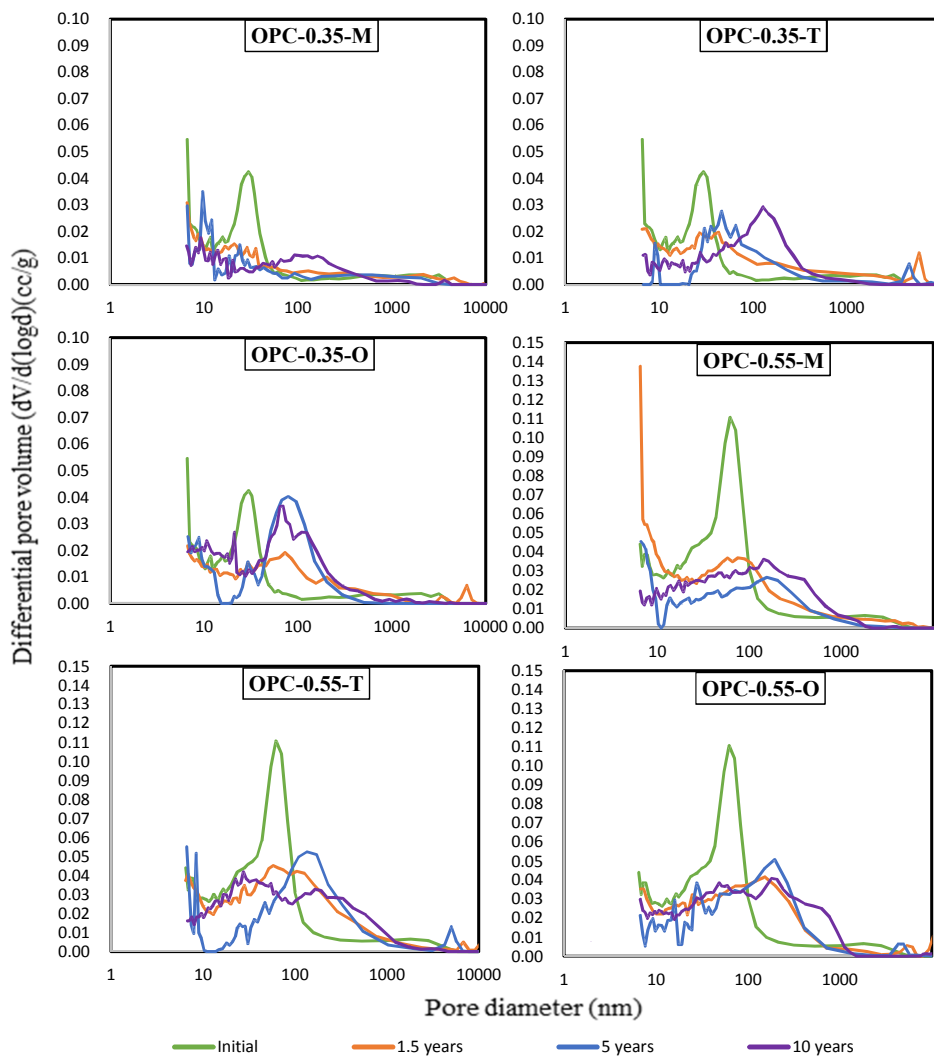

Fig. 3 The characteristic curves of the differential pore volume as a function of pore diameter for cement-based mortars in Series 1. (Note: V is the pore volume and d is the equivalent pore diameter; OPC- identifies the cement type; 0.35 and 0.55 – are the water-to-cement ratio; M, T and O identify Muroran, Tokyo and Okinawa, respectively).
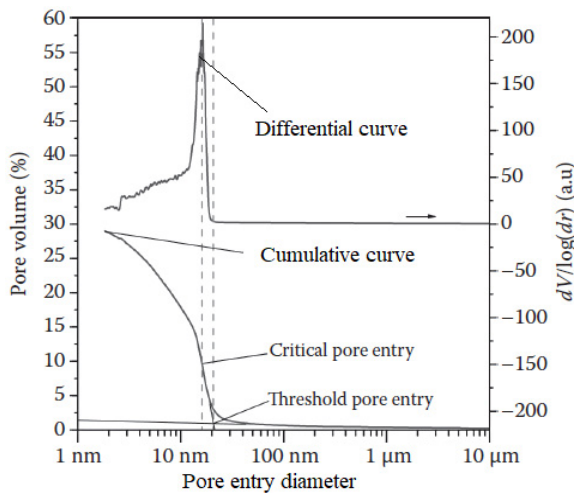
Fig. 13 The determination of the critical pore entry diameter and threshold pore entry diameter from the cumulative and differential curve (Scrivener *et al*. 2016).

paring the differential curves of OPC-0.35-M and OPC-0.55-M (or OPC-0.35-T and OPC-0.55-T or OPC-0.35-O and OPC-0.55-O, respectively) in **Fig. 3,** it can be found that the highest peak is higher with increasing W/C ratio. Furthermore, the higher the temperature of the exposure area, the sharper the peak of the differential pore size distribution curves in case of OPC-0.35. The diameter envelopes and the increased pore volume show that the exposure samples have a coarser pore size than the initial curing samples. The coarsened pore structure most probably resulted from the increased temperature, as confirmed by the differences in the weather conditions of the exposure sites. The coarsening pore structure results are in general agreement with previous work (Rostásy *et al*. 1980). The drying process causes the coarser the pore structure and a significant compression of the cement gel. In addition, the formation of large amounts of inkbottle pores due to the drying process reveals the change of the pore structure (Espinosa and Franke 2006). The amount of capillary

pores, i.e, the 40–2000 nm pore size range, and the total pore volume increase mention a large coarsening of the pore structure.

Results of the pore volume change for each pore size range are summarized in **Fig. 4**. As can be seen in **Fig. 4**, the effect of the curing and exposure conditions cause significant changes in the pore volume of mortar for Series 1. For OPC-0.55 mortar, the pore volumes of the 10-year exposure mortar samples (M, T, and O) are higher than in the case of initial curing only (4WK). On the other hand, the pore volume of the 10-year exposure mortar samples (M) decreases and is nearly lower than initial curing only (4WK) for OPC-0.35 mortar. Furthermore, the pore volumes of specimens OPC-0.55 and OPC-0.35, which were cured at 50°C in the laboratory, are considerably higher than those of the 10-year exposure specimens (M, T, and O). High curing temperature does affect the pore structure change in a significant way, increasing the pore volume of large capillary pores. This effect is much more important in the range 40–2000 nm. Analysis of the incremental pore size distribution data shows that the laboratory curing mortar specimen has a much higher proportion of pore sizes with diameters in the range of 40–2000 nm than the 10-year exposure specimens (M, T, and O). The volume of these pores apparently increased with increasing W/C ratio. Previous studies (Atarashi *et al*. 2009; Kamada *et al*. 1996; Nakamura *et al*. 2015a; Nakamura *et al*. 2015b) have shown that the volume of pores of diameter 40–2000 nm significantly affects the mechanism of frost damage in cement-based materials. Therefore, pore sizes in this range must be taken into account when analyzing the pore structure change of cement-based materials. The change in volume of the aforementioned pores is presented in Section 3.2.

In Series 2, the effect of the relative humidity on the pore structure change was examined. **Figure 5** shows the differential pore size distribution of mortar at 50°C corresponding to the increase of the relative humidity. In general, the curves show the envelope of differential
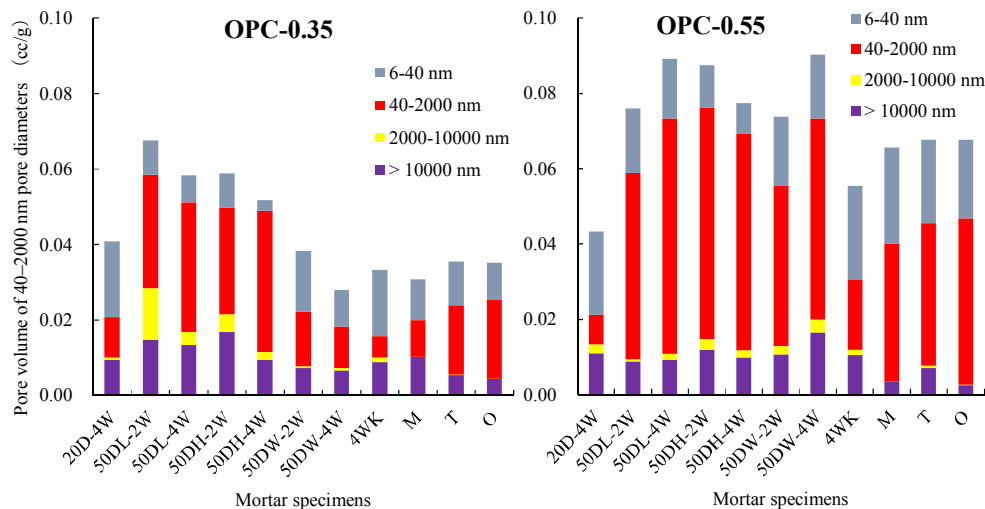

Fig. 4 Influence of the environmental conditions on the pore volume of mortar in Series 1.

pore size distributions for OPC-0.35 mortars, which were measured at 0, 4, 8, 13, and 26 weeks. From the differential pore size distribution shown in **Fig. 5**, the 26-w mortar presents the highest derivative peak with a pore diameter of approximately 100 nm (except for 75%RH and 100% RH). By observing the pore size distribution, the critical pore entry diameter is found to be obviously larger, expanding from 10 nm at initial curing to 100 nm at 26-w curing. A larger critical pore entry diameter indicates that the pore is coarser. Furthermore, it is clear that the highest derivative peak strongly decreases as the relative humidity increases, especially for the 50°C and 100% RH mortar. The results in **Fig. 5**

clearly show that the highest derivative peak dropped sharply when the relative humidity reached 75% RH and it could not observe in case of in water (100% RH). It is interesting that the differential pore volume does not change in water. Based on these observations, it can be concluded that the relative humidity has a significant effect on the pore structure change of mortar. In other words, the pore structure change is a function of relative humidity. This conclusion agrees with that of other investigations (Adolphs *et al*. 2002). The gel pores remain continuously water-filled. Furthermore, at intermediate and low relative humidity, the capillary pressure works in the water-filled pulling the pore walls together. Beau-
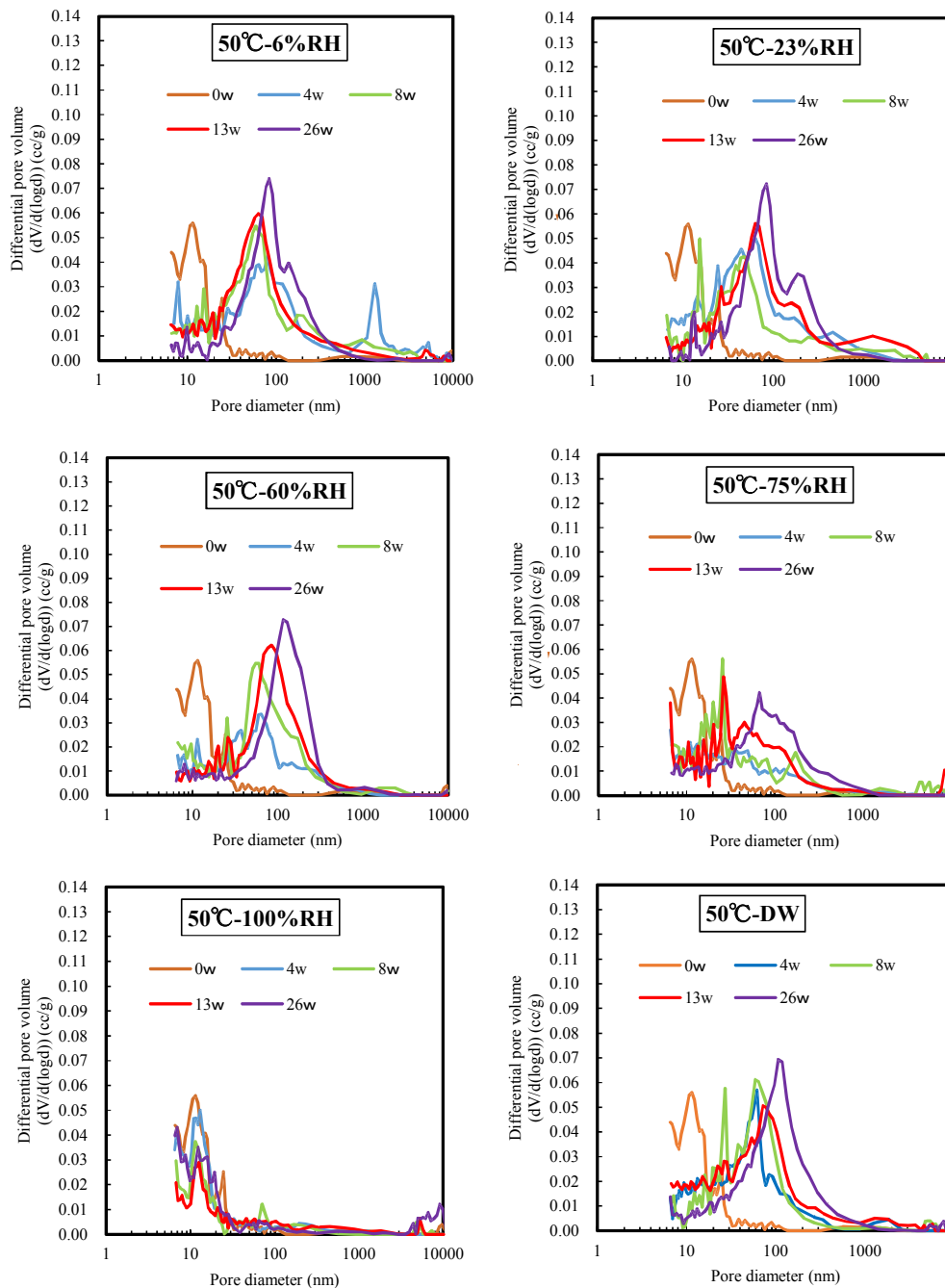

Fig. 5 Differential pore size distribution for OPC-0.35 mortar in Series 2.

doin and Tamtsia (2004) pointed out that the microstructural change of C-S-H is influenced by drying at a low and intermediate humidity and the collapse of the C-S-H structure due to drying may occur. This is the reason for the coarsening of the pore structure at lower relative humidity.

3.2 Pore structure change in the diameter range of 40 to 2000 nm due to temperature and relative humidity

First, comparing the volume of the pores of diameter 40–2000 nm in environmental conditions (PV_d) and the volume of the pores of diameter 40–2000 nm in initial curing (PV_i) in Series 1 shows that the change of the pore volume in the 40–2000 nm range tends to reach an upper limit due to exposure time in case of OPC-0.55 (see **Fig. 6(b)**). The significant increase rate of the changes in the pore volume for the O site samples are particularly faster than for the M and T climate exposure sites. A clear difference in the rate of volume change can be observed in the case of OPC-0.35 (see **Fig. 6(a)**). **Figure 6(a)** shows an obviously faster rate of increase in volume change during the first 5 years of exposure, whereas the rate of increase slowed down for the following 5 years. For OPC-0.55 mortar, the pore volume of mortar in the 40–2000 nm diameter range at the O site increased by a factor of approximately 2 during the first 5 years of exposure, after which the increase significantly slowed down with almost no change for the subsequent 5 years. As such, it can be concluded that the higher the temperature, the greater the rate of pore volume change for the pore size range of 40–2000 nm. Furthermore, the pore volume in this range can reach a limiting value after long-term exposure.

In addition, our results in Series 1 provide compelling evidence for the pore structure change of 40–2000 nm pore size range due to long-term exposure but they may still not be sufficient. An increase in environmental temperature highly influences the deterioration processes of cement-based materials (Bastidas-Arteaga *et al*. 2010, 2013; Stewart *et al.* 2011; Yoon *et al*. 2007). The deterioration such as frost damage can be affected by the pore structure change of 40–2000 nm pore size range. The frost resistance is higher with lower amount

of pore in the 40–2000 nm pore size range (Kamada *et al*. 1996). Therefore, this study provides a framework for future studies. Future work should therefore include a follow-up designed to evaluate the influence of the pore structure change of 40–2000 nm pore size range on frost resistance in the long term for different climate regions.

Figure 7 shows the linear correlation between the change in the pore volume for 40–2000 nm pore diameters and the environmental conditions in Series 1, i.e., the temperature and relative humidity for outdoor exposure and for in-laboratory curing. **Figure 7** also shows that there exists a meaningful correlation between the volume of pores in the 40–2000 nm diameter range and the temperature as well as between the same pore volume and the relative humidity. The tendency is clearly illustrated in **Figs. 7(a)** and **(b)**. The linear correlation in **Fig. 7(a)** has the best fit for the experimental data. For the case of the OPC-0.35 mortar specimens, **Fig. 7(a)** indicates that the pore volume of the pores of diameter 40–2000 nm exhibits the highest correlation with the temperature, with a coefficient of determination R^2 reaching 0.984. For both OPC-0.35 and OPC-0.55, there is an upward trend in the volume of the pores of diameter 40–2000 nm with increasing temperature and increasing W/C (see **Fig. 7(a)**, except for 20D-4W), which is in agreement with similar experiments performed by Nakamura *et al*. (2015b). However, unlike previous investigations that were only concerned about the effect of the temperature, in this study, the effect of the relative humidity on the volume of the pores of diameter 40–2000 nm is also observed. The results illustrated in **Fig. 7(b)** highlight that the pore volume decreases with an increase in the relative humidity. Alternatively, it can be anticipated that the linear correlation line may meet the 4WK line at 100% RH. Meanwhile, the volume of 40–2000 nm diameter pores does not change in water.

Finally, an interesting observation in this study is that the pore volume changes due to both temperature and relative humidity in Series 2, as shown in **Figs. 8** and **9**. The results in **Fig. 8** show that the temperature increases with increasing pore volume. In most cases, the 40–2000 nm pore volume started to increase after 2 weeks, then dramatically increased and reached the highest
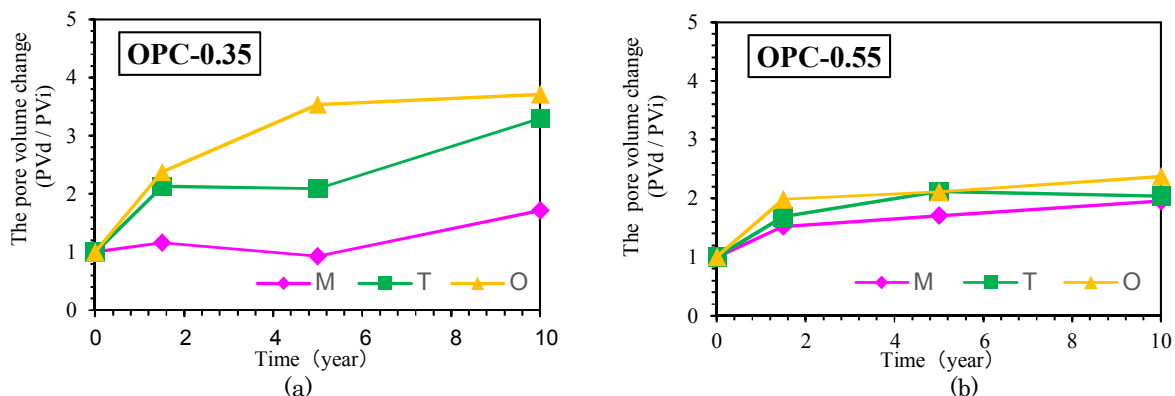

Fig. 6 Pore volume change of the 40-2000 nm-diameter pores of mortar after 10 years of outdoor exposure in Series 1.

value, close to the upper limit, after about 13 weeks. This is similar to the trends seen in Nakamura *et al.* (2015b). These observations are important since they refine findings in the literature concerning the influence of temperature on the 40–2000 nm diameter pore volume. Previous studies (Nakamura *et al.* 2015a; Nakamura *et al.* 2015b) have identified the high drying temperature as a reason for the coarsening of pore structures. However, the results presented in this paper show that the relative humidity is another factor contributing to the coarseness of the pore structure, and as shown in **Fig. 9**, this contribution can be significant. A significant difference in the pore volume change is observed, as seen in **Fig. 9**, where the volume of the pores of diameter 40–

2000 nm increases with decreasing relative humidity. For the 6% RH, 23% RH, 60% RH, and DW mortars, there was a very rapid increase in the pore volume after 2 weeks; the pore volume then slowly increased after 4 weeks and remained constant after about 13 weeks. The volume of the pores of diameter 40–2000 nm increased slightly for the 75% RH mortar for case OPC-0.35-50°C. Interestingly, the pore volume does not change in most cases for the 100% RH mortar during the curing period. Therefore, the results in **Figs. 8** and **9** show the need to consider both of relative humidity and temperature for predicting the change of pore volume of diameter 40–2000 nm pores in mortar. Based on the temperature and humidity dependency of the pore structure change, the
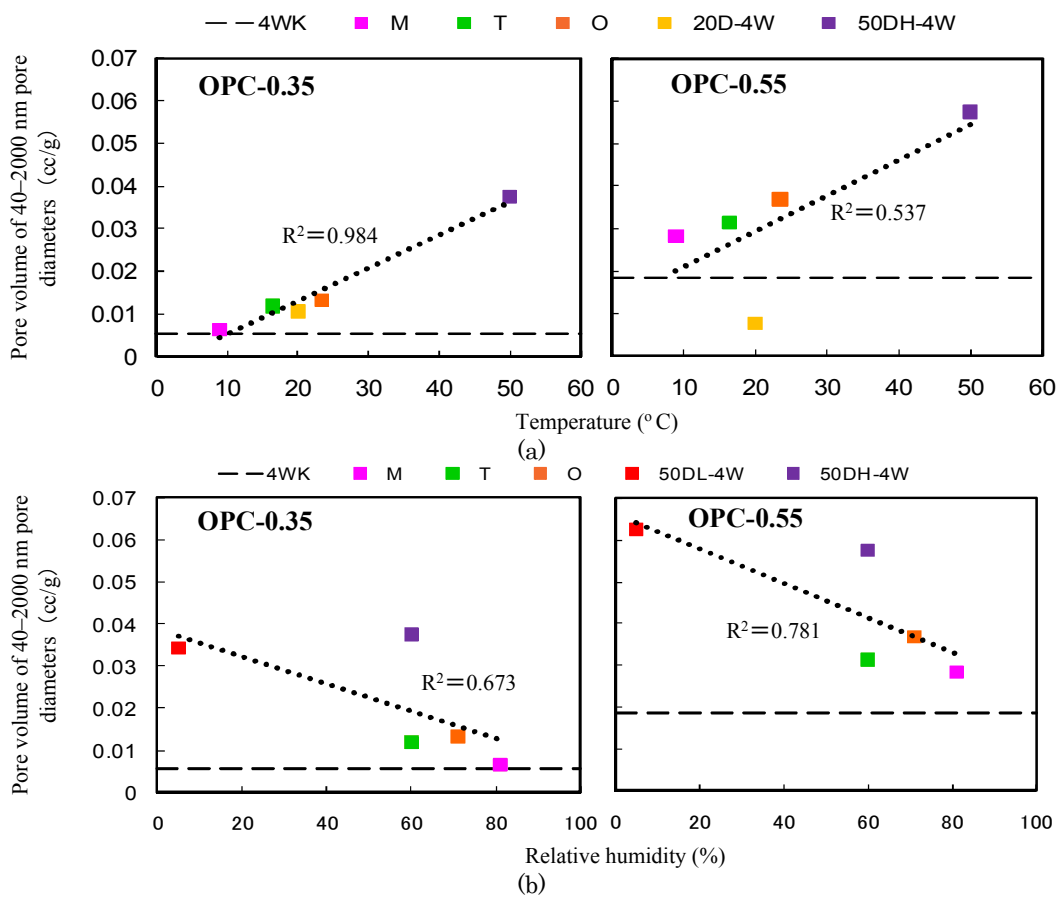

Fig. 7 Change in pore volume of the 40-2000 nm-diameter pores due to (a) temperature and (b) humidity in Series 1.
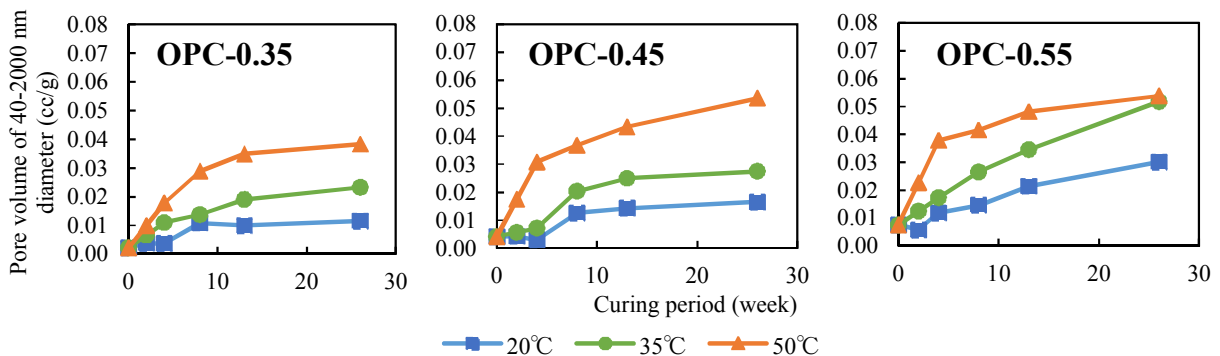

Fig. 8 Effect of curing temperature on the pore volume of the 40–2000 nm-diameter pores of mortar in Series 2.

datum humidity and datum temperature were considered. These parameters will be discussed in detail in Section 3.3.

3.3 Relationship between the structure change of 40–2000 nm pores and the modified maturity function

As is well known, according to the origins of the maturity method (Nurse 1949; Saul 1951), maturity is calculated using the Nurse-Saul maturity equation (see Eq. (1)); nevertheless, this equation is only applied for the strength prediction of concrete. It was suggested in the introduction that the pore structure change is closely related to the maturity function. There are very few results in the scientific literature about this relation. Nakamura *et al.* (2015a,b) found an empirical formula expressing the relation between the pore structure change and the maturity:

$$P_d = 0.0012\sqrt{M_p} + 0.0097 \quad \left(0 \le M_p < 598\right)$$
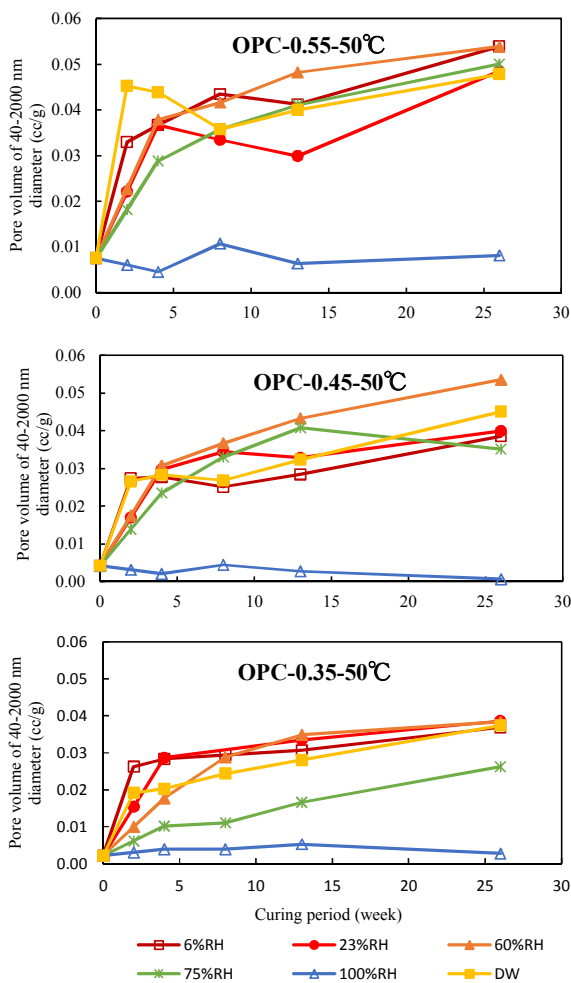$$P_d = 0.0391 \quad \left(M_p \ge 598\right)$$
(2)

Fig. 9 Effect of relative humidity on the pore volume of the 40–2000 nm-diameter pores of mortar in Series 2.

where P_d is the pore volume of pores with 40–2000 nm diameters after drying (cc/g) and M_p is the maturity (°C·days). M_p, which is a function of the drying temperature corresponding to the pore structure change, is given as

$$M_p = \sum_{t=1}^{n} \left(\theta_{d,t} - 31\right)\Delta t$$
(3)

where $\theta_{d,t}$ is the curing temperature (°C) and t is the time (days).

The function in Eq. (2) shows a strong correlation between the drying temperature and the pore structure change. Nonetheless, the maturity in Eqs. (2) and (3) does not include the relative humidity, as Eq. (3) considers time and temperature as the only main factors. It is clear that the environmental conditions, including both temperature and humidity, strongly affect the pore structure change. The results in this study point to the need to consider the effect of relative humidity on the pore structure change as an equally major factor. This is in agreement with a study by Liao *et al.* (2008) in which it was concluded that the relative humidity needs to be accounted for when using a maturity function for concrete strength prediction. Therefore, it is necessary to improve these equations to establish proper and complete expressions of the pore structure change.

The correlation between the change in the volume of the pores of diameter 40–2000 nm and the modified maturity can be illustrated in general by the following formula:

$$PV_d = \alpha\sqrt{M_{ph}} + \beta \quad \left(0 \le \sqrt{M_{ph}} < \sqrt{a}\right)$$
$$P_d = \gamma \quad \sqrt{M_{ph}} \ge \sqrt{a}$$
(4)

where α is the slope of a straight line to the upper limit, β is the initial pore volume (cc/g) value before drying, γ is the upper limit of the pore volume (cc/g), and a is an empirical constant. Based on the experimental results in Series 2, all of these parameters can be expressed by a linear equation from a linear correlation with the W/C ratio:

$$\alpha = 0.002(\frac{W}{C}) + 0.0005$$
(5)

$$\beta = 0.027(\frac{W}{C}) - 0.0076$$
(6)

$$\gamma = 0.0695(\frac{W}{C}) + 0.0062$$
(7)

$$a = 372.4(\frac{W}{C}) + 307.67$$
(8)

In this study, we propose the modified maturity function (M_{ph}) based on the results in Series 2, which is a function of temperature and humidity, expressed as the

following equation:

$$M_{ph} = \sum_{t=1}^{n} \Delta RH_t \left(\theta_{d,t} - D_t \right) \Delta t \tag{9}$$

where $\theta_{d,t}$ is the curing environment temperature (°C), D_t is the datum temperature at which the further increase of the volume of the pores of diameter 40–2000 nm does not occur (°C), t is the time (days), and ΔRH_t is the added humidity factor. ΔRH_t is

$$\Delta RH_t = \left(H_t - \varphi_{d,t} \right) \tag{10}$$

where $\varphi_{d,t}$ is the curing environment humidity and H_t is the datum humidity at which the further increase of the volume of the pores of diameter 40–2000 nm does not occur (% RH).

The datum temperature and datum humidity in Eqs. (9) and (10) were obtained based on **Fig. 10**. The datum temperature in Eq. (9) is the temperature corresponding to the highest coefficient of determination at which the further increase of the volume of the pores of diameter 40–2000 nm does not occur, as shown in **Fig. 10(a)**. The coefficient of determination was obtained by the correlation between the change in the volume of the pores of diameter 40–2000 nm and the modified maturity. It is interesting to see that the datum temperature in Eq. (9) is 16°C for all W/C cases (see **Fig. 10(a)**). Similarly, the
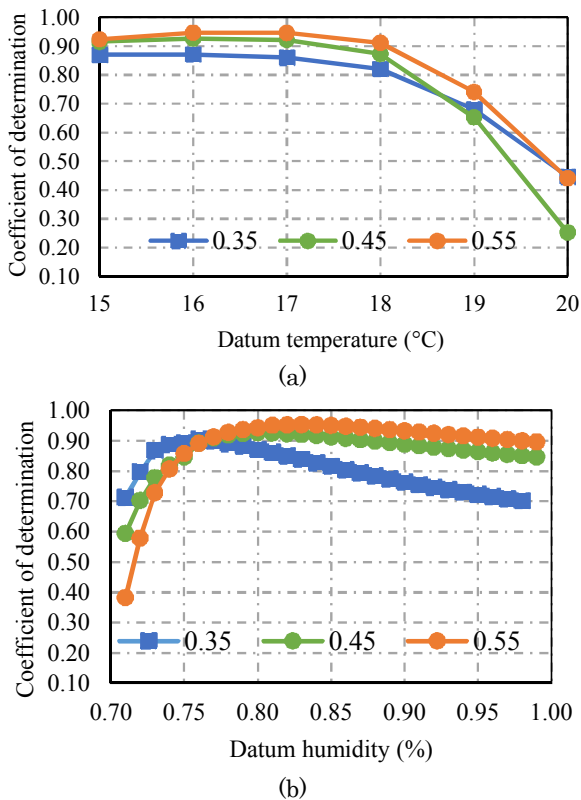
datum humidity in Eq. (10) is the humidity corresponding to the highest coefficient of determination at which the further increase of the volume of the pores of diameter 40–2000 nm does not occur was determined for each W/C. For W/C = 0.35, 0.45, and 0.55, the datum humidity was 76% RH, 80% RH, and 83% RH, respectively (see **Fig. 10(b)**).

Figure 11 indicates the relationship between the volume of the pores of diameter 40–2000 nm and the modified maturity which as a function of temperature and

Fig. 10 Coefficient of determination of the modified maturity formula for each datum temperature and datum humidity.
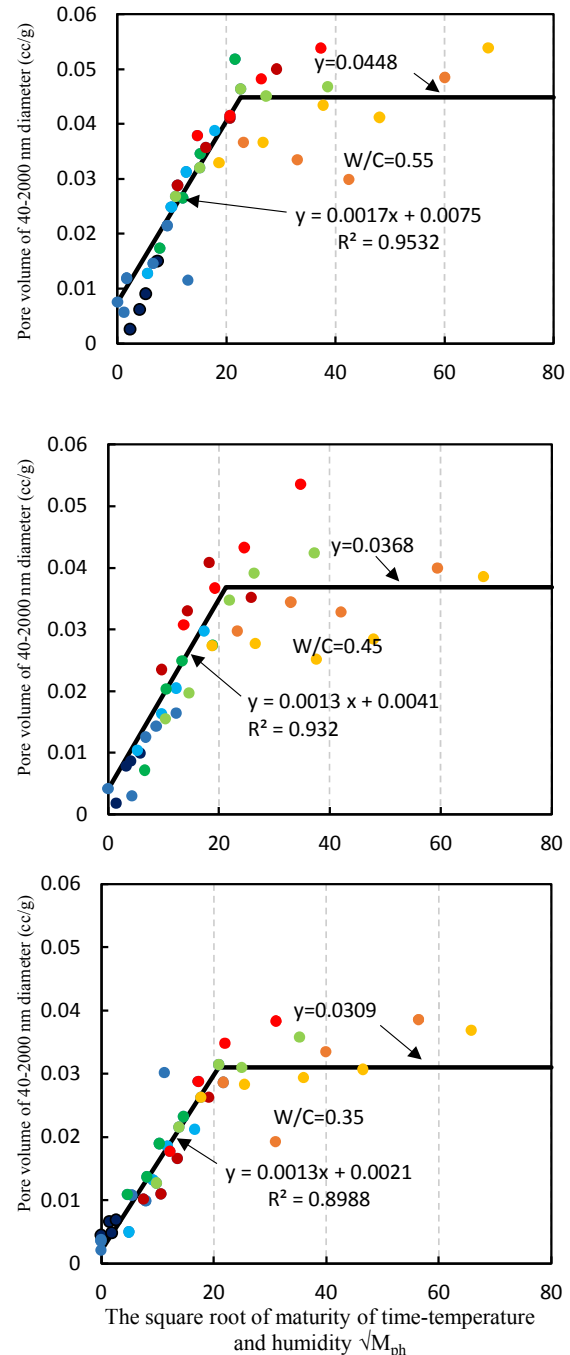

Fig. 11 The pore volume of the 40-2000 nm-diameter pores changing as a function of the square root of the modified maturity.

relative humidity. It can be clearly seen that the line has a steep slope, which was measured over the square root of the modified maturity. An empirical formula can be obtained from the initial slope of the line, which shows a good correlation between the pore volume and the modified maturity of each W/C ratio (see Eq. (4)). The volume of the pores of diameter 40–2000 nm soon reached a maximal value (the so-called upper limit), at which most of the data converges to a straight line with a different upper limit value. The higher the W/C ratio, the larger the upper limit. As can be seen from **Fig. 11**, it is clear that the coefficient of determination R^2 reached a higher value with increasing W/C ratio. It can be concluded that the W/C ratio has a significant impact on the volume of the pores of diameter 40–2000 nm. In agreement with the literature (Nakamura *et al*. 2015a; Nakamura *et al*. 2015b), this study found that the modified maturity has a close relationship with the pore structure of mortar. The relationship between the change of volume of the pores of diameter 40–2000 nm and the modified maturity due to laboratory and exposure condition is shown in **Fig. 12**. It can be seen that the correlation is good in both case of laboratory and exposure condition. The change of volume of the pores of diameter 40–2000

nm due to laboratory is higher than the change of volume of the pores of diameter 40–2000 nm due to exposure condition. Similar upward trends of the change of volume of the pores of diameter 40–2000 nm are observed here for OPC-0.35 and OPC-0.55. Therefore, it can be understood that the pores of diameter 40–2000 nm was coarsened due to environment condition.

To sum up, the application of Eq. (4) to predict the change of volume of the pores of diameter 40–2000 nm based on modified maturity and the limits of this work open new perspectives for the future work. The prediction equation of the current study investigated pore structure with only 40–2000 nm range. However, this pore size range strongly affects the frost resistance of cement-based materials according to Kamada (1996). Therefore, the application of Eq. (4) to predict frost damage needs to be taken into consideration.

4. Conclusions

The experimental results support the following conclusions:
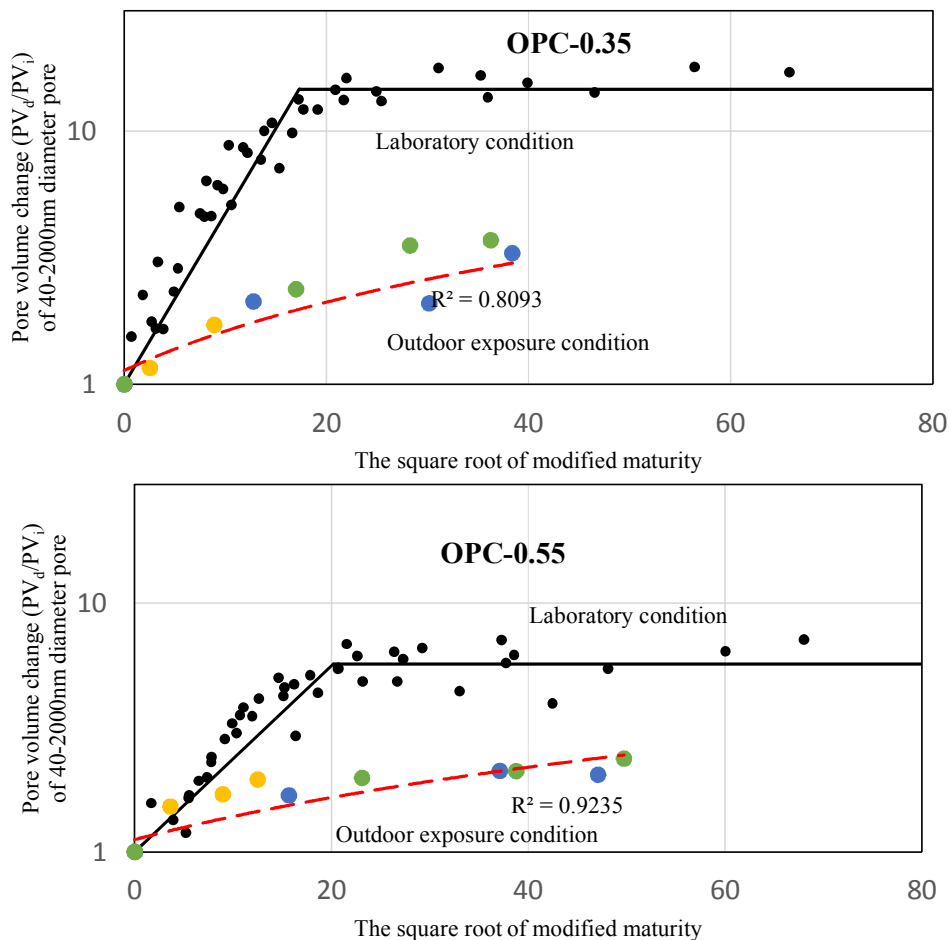1) Both the laboratory and outdoor exposure tests revealed that the pore structure of mortar was coars-

Fig. 12 The relationship between the change of pore volume of the 40-2000 nm-diameter pores and the modified maturity of mortar due to laboratory and outdoor exposure condition. (The black dot corresponds to laboratory condition and the color dot corresponds to exposure condition)

ened due to temperature and relative humidity; the volume of the pores of diameter 40–2000 nm increased and reached an upper limit value.

2) The drying temperature was more critical to the coarsening of the pore structure. The influence of drying on the pore structure change at 50°C was more severe than the effects of the outdoor exposure test on the mortar specimens.

3) The relative humidity had a significant effect on the pore structure change of mortar. The pore volume of the 40–2000 nm diameter pores increased with decreasing relative humidity. The pore volume after initial curing did not change in water content.

4) A modified maturity function, which can predict the pore structure change due to temperature and relative humidity, was proposed based on the experimental results. The function shows a meaningful correlation between the volume of the pores of diameter 40–2000 nm and the temperature and relative humidity.

5) The higher the W/C ratio, the higher the upper limit value of the pore volume change.

Acknowledgements

References

Abdel-Jawad, Y. A., (2006). "The maturity method: Modifications to improve estimation of concrete strength at later ages." *Construction and Building Materials*, 20(10), 893-900.

ACI 116R-00, (2002). *"Cement and concrete terminology (Reapproved 2005)."* American Concrete Institute.

Adolphs, J., Setzer, M. J. and Heine, P., (2002). "Changes in pore structure and mercury Contact angle of hardened cement paste depending on relative humidity." *Materials and Structures*, 35(8), 477-86.

Aligizaki, K. K., (2006). *"Pore structure of cement-based materials: Testing, interpretation and requirements."* Taylor & Francis.

Aono, Y., Matsushita, F., Shibata, S. and Hama, Y., (2007). "Nano-structural changes of C-S-H in hardened cement paste during drying at 50°C." *Journal of Advanced Concrete Technology*, 5(3), 313-23.

Aono, Y., Matsushita, F., Shibata, S. and Hama, Y., (2006). "Study on frost resistance and its degradation mechanism of concrete subjected to drying and wetting cycles." *Journal of Structural and Construction Engineering (Transactions of AIJ)*, 71(607), 15-22.

ASTM C1074 - 11, *"Standard Practice for Estimating Concrete Strength by the Maturity Method."* ASTM International.

Atarashi, D., Hama, Y., Shibuya, M. and Aono, Y., (2009). "Changes of pore structure and frost resistance of mortar during drying or wetting-drying." *Cement Science and Concrete Technology*, 63(1), 155-60.

Bastidas-Arteaga, E., Chateauneuf, A., Sánchez-Silva, M., Bressolette, P. and Schoefs, F., (2010). "Influence of weather and global warming in chloride ingress into concrete: A stochastic approach." *Structural Safety*, 32(4), 238-49.

Bastidas-Arteaga, E., Schoefs, F., Stewart, M. G. and Wang, X., (2013). "Influence of global warming on durability of corroding RC structures: A probabilistic approach." *Engineering Structures*, 51(June), 259-66.

Beaudoin, J. J. and Tamtsia, B. T., (2004). "Effect of drying methods on microstructural changes in hardered cement paste: an A.C. impedance spectroscopy evaluation" *Journal of Advanced Concrete Technology*, 2(1), 113-120.

Carino, N. J. and Tank, R. C., (1992). "Maturity functions for concretes made with various cements and admixtures." *ACI Materials Journal*, 89(2), 188-96.

Chang, H., Mu, S., Xie, D. and Wang, P., (2017). "Influence of pore structure and moisture distribution on chloride 'maximum Phenomenon' in surface layer of specimens exposed to cyclic drying-wetting condition." *Construction and Building Materials*, 131, 16-30.

Choi, Y. C., Kim, J. and Choi, S., (2017). "Mercury intrusion porosimetry characterization of micropore structures of high-strength cement pastes incorporating high volume ground granulated blast-furnace slag." *Construction and Building Materials*, 137, 96-103.

Cook, R. A. and Hover, K. C., (1999). "Mercury porosimetry of hardened cement pastes." *Cement and Concrete Research*, 29(6), 933-43.

Diamond, S., (2000). "Mercury porosimetry: An inappropriate method for the measurement of pore size distributions in cement-based materials." *Cement and Concrete Research*, 30(10), 1517-25.

Kamada, E., Senbu, O., Tabata, M. and Tanaka, H., (1996). "Statistical investigation concerning the effects of pore structure on the frost resistance of concrete." *Journal of Structural and Construction Engineering*, No. 487, 1-9.

Espinosa, R. M. and Franke, L., (2006). "Influence of the age and drying process on pore structure and sorption isotherms of hardened cement paste." *Cement and Concrete Research*, 36(10), 1969-84.

Galan, I., Beltagui, H., García-Maté, M., Glasser, F. P. and Imbabi, M. S., (2016). "Impact of drying on pore structures in ettringite-rich cements." *Cement and Concrete Research*, 84, 85-94.

Gallé, C., (2001). "Effect of drying on cement-based materials pore structure as identified by mercury intrusion porosimetry: A comparative study between oven-, vacuum-, and freeze-drying." *Cement and Concrete Research*, 31(10), 1467-77.

Galobardes, I., Cavalaro, S. H., Goodier, C. I., Austin, S. and Rueda, Á., (2015). "Maturity method to predict the evolution of the properties of sprayed concrete." *Construction and Building Materials*, 79, 357-69.

Gao, Y., Wu, K. and Jiang, J., (2016). "Examination and modeling of fractality for pore-solid structure in cement paste: Starting from the mercury intrusion porosimetry test." *Construction and Building Materials*, 124, 237-43.

Hamami, A. A., Turcry, P. and Aït-Mokhtar, A., (2012). "Influence of mix proportions on microstructure and gas permeability of cement pastes and mortars." *Cement and Concrete Research*, 42(2), 490-98.

Jin, N. J., Seung, I., Choi, Y. S. and Yeon, J., (2017). "Prediction of early-age compressive strength of epoxy resin concrete using the maturity method." *Construction and Building Materials*, 152, 990-98.

Lamond, J. F. and Pielert, J. H., (2006). "*Significance of tests and properties of concrete and concrete-making materials*." ASTM.

Liao, W.-C., Lee, B. J. and Kang, C. W., (2008). "A humidity-adjusted maturity function for the early age strength prediction of concrete." *Cement and Concrete Composites*, 30(6), 515-23.

Malhotra, V. M. and Carino, N. J., (2004). "*Handbook on nondestructive testing of concrete*." 2nd ed. CRC Press.

Marusin, S., (1981). "The effect of variation in pore structure on the frost resistance of porous materials." *Cement and Concrete Research*, 11(1), 115-24.

Maruyama, I., Sakamoto, N., Matsui, K. and Igarashi, G., (2017). "Microstructural changes in white portland cement paste under the first drying process evaluated by WAXS, SAXS, and USAXS." *Cement and Concrete Research*, 91, 24-32.

McIntosh, J. D., (1949). "Electrical curing of concrete." *Magazine of Concrete Research*, 1(1), 21-28.

Meneghetti, F. and Meneghetti, T., (1985). "Non-destructive testing to evaluated in situ maturity on prestressed reinforced concrete members." *Materials and Structures*, 18(3), 171-80.

Moukwa, M. and Aïtcin, P.-C., (1988). "The effect of drying on cement pastes pore structure as determined by mercury porosimetry." *Cement and Concrete Research*, 18 (5), 745-52.

Nakamura, T., Hama, Y. and Taniguchi, M., (2015). "Relationship between the change of volume of pore size 40-2000nm diameter macro pore of mortar in drying condition and maturity." *Journal of Structural and Construction Engineering (Transactions of AIJ)*, 80(713). Japan, 981-89.

Nakamura, T., Hama, Y. and Zakaria, M., (2015). "Influence of environmental conditions on pore structure change in mortar with various types of cement." In *Durability of Reinforced Concrete from Composition to Protection*, 155-67. Springer International Publishing.

Neville, A. M., (2012). "*Properties of concrete*." 5th ed.

Harlow, England: Prentice Hall, Pearson.

Nurse, R. W., (1949). "Steam curing of concrete." *Magazine of Concrete Research*, 1(2), 79-88.

Mehta, P. M. and Monteiro, P. J. M., (2014). "*Concrete: microstructure, properties, and materials*." 4th ed. New York: McGraw-Hill Education.

Parrott, L. J., (1981). "Effect of drying history upon the exchange of pore water with methanol and upon subsequent methanol sorption behaviour in hydrated alite paste." *Cement and Concrete Research*, 11(5), 651-58.

Parrott, L. J., (1992). "Variations of water absorption rate and porosity with depth from an exposed concrete surface: Effects of exposure conditions and cement type." *Cement and Concrete Research*, 22(6), 1077-88.

Powers, T. C., (1958). "Structure and physical properties of hardened Portland cement paste." *Journal of the American Ceramic Society*, 41(1), 1-6.

Powers, T. C. and Brownyard, T. L., (1946). "Studies of the physical properties of hardened portland cement paste." *ACI Journal Proceedings*, 43(9), 469-504.

Reinhardt, H.-W. and Stegmaier, M., (2006). "Influence of heat curing on the pore structure and compressive strength of self-compacting concrete (SCC)." *Cement and Concrete Research*, 36(5), 879-85.

Rostásy, F. S., Weiβ, R. and Wiedemann, G., (1980). "Changes of pore structure of cement mortars due to temperature." *Cement and Concrete Research*, 10(2), 157-64.

Saul, A. G. A., (1951). "Principles underlying the steam curing of concrete at atmospheric pressure." *Magazine of Concrete Research*, 2(6), 127-40.

Scrivener, K., Snellings, R. and Lothenbach, B., (2016). "*A practical guide to microstructural analysis of cementitious materials*." Taylor & Francis.

Stewart, M. G., Wang, X. and Nguyen, M. N., (2011). "Climate change impact and risks of concrete infrastructure deterioration." *Engineering Structures*, 33(4), 1326-37.

Taylor, H. F. W., (1997). "*Cement chemistry*." T. Telford.

Tonoli, G. H. D., Santos, S. F., Savastano, H., Delvasto, S., de Gutiérrez, R. M. and de Murphy, M. M., (2011). "Effects of natural weathering on microstructure and mineral composition of cementitious roofing tiles reinforced with fique fibre." *Cement and Concrete Composites*, 33(2), 225-32.

Topçu, İ. B. and Toprak, M. U., (2005). "Fine aggregate and curing temperature effect on concrete maturity." *Cement and Concrete Research*, 35(4), 758-62.

Voigt, T., Sun, Z. and Shah, S. P., (2006). "Comparison of ultrasonic wave reflection method and maturity method in evaluating early-age compressive strength of mortar." *Cement and Concrete Composites*, 28(4), 307-16.

Volz, C. K., Tucker, R. L., Burns, N. H. and Lew, H. S., (1981). "Maturity effects on concrete strength." *Cement and Concrete Research*, 11 (1), 41-50.

Winslow, D. and Liu, D., (1990). "The pore structure of paste in concrete." *Cement and Concrete Research*, 20(2), 227-35.

Xuan, D., Zhan, B. and Poon, C. S., (2018). "A maturity approach to estimate compressive strength development of CO_2-cured concrete blocks." *Cement and Concrete Composites*, 85, 153-60.

Yikici, T. A. and Chen, H.-L., (2015). "Use of maturity method to estimate compressive strength of mass concrete." *Construction and Building Materials*, 95, 802-12.

Yoon, I.-S., Çopuroğlu, O. and Park, K.-B., (2007). "Effect of global climatic change on carbonation progress of concrete." *Atmospheric Environment*, 41(34), 7274-85.

Zhang, S. and Zhang, M., (2006). "Hydration of cement and pore structure of concrete cured in tropical environment." *Cement and Concrete Research*, 36(10), 1947-53.